# Mission-Profile-Based System-Level Reliability Analysis in DC Microgrids

Peyghami, Saeed; Wang, Huai; Davari, Pooya; Blaabjerg, Frede

*Published in:*
I E E E Transactions on Industry Applications

*DOI (link to publication from Publisher):*
10.1109/TIA.2019.2920470

*Publication date:*
2019

*Document Version*
Accepted author manuscript, peer reviewed version

This article has been accepted for publication in a future issue of this journal, but has not been fully edited. Content may change prior to final publication. Citation information: DOI 10.1109/TIA.2019.2920470, IEEE Transactions on Industry Applications

# Mission Profile based System-level Reliability Analysis in DC Microgrids

Saeed Peyghami, *Member, IEEE*, Huai Wang, *Senior Member, IEEE*,
Pooya Davari, *Senior Member, IEEE*, and Frede Blaabjerg, *Fellow, IEEE*
Department of Energy Technology, Aalborg University, Aalborg 9220 East, Denmark
{sap,hwa,pda,fbl}@et.aau.dk

***Abstract* – Mission profiles such as environmental and operational conditions together with the system structure including energy resources, grid and converter topologies induce stress on different converters and thereby play a significant role on power electronic systems reliability. Temperature swing and maximum temperature are two of the critical stressors on the most failure prone components of converters, i.e., capacitors and power semiconductors. Temperature related stressors generate electro-thermal stress on these components ultimately triggering high potential failure mechanisms. Failure of any component may cause converter outage and system shutdown. This paper explores the reliability performance of different converters operating in a power system and indicates the failure prone converters from wear out perspective. It provides a system-level reliability insight for design, control and operation of multi-converter system by extending the mission profile-based reliability estimation approach. The analysis is provided for a dc microgrid due to the increasing interest that dc systems have been gaining in recent years; however, it can be applied for reliability studies in any multi-converter system. The outcomes can be worthwhile for maintenance and risk management as well as security assessment in modern power systems.**

***Index Terms* – reliability, mission profile, system architecture, dc microgrid, lifetime, energy management, critical stressor, application-specific reliability.**

## I. INTRODUCTION

Power electronics are the key enabling technology in a wide range of applications comprising of smart-grids, e-mobility, aerospace, energy transmission systems, consumer electronics, and lighting. The increasing use of power electronic converters in modern electrical systems brings new reliability challenges, in terms of accumulated failure, availability, and maintenance. Therefore, reliability analysis of power electronic converter intensive system is one of the important tools to support the model-based decision-making and to identify key design variables, e.g., environmental and operational factors.

Reliability of an engineering system is the probability that the system meets some specified demands under specified environmental conditions [1]. A power electronics system is a cluster of power converters including various components in its power stage. The failure of an individual component may cause the system to shut down. Therefore, identifying fragile components, their stressors and understanding their failure mechanisms are essential for modern power system reliability assessment.

Semiconductors and capacitors are known as the most fragile components of power converters [2], [3]. The component failure occurs once the applied stress exceeds the corresponding strength. The main critical stressor for these components is the temperature related stress comprising of high temperature and temperature cycling. The thermal stress can be induced by mission profile, system architecture and control strategy. Mission profile can be divided into environmental conditions – such as solar irradiance, wind speed, ambient temperature, and humidity – and operational conditions (e.g., load profile). Furthermore, the system architecture includes type of energy resources, converter topologies, and grid structures – such as ac grid, dc grid, etc. Depending on the application and corresponding architecture, the applied control strategy such as voltage and current controllers, modulation scheme, maximum power point tracking (MPPT) approaches for a single unit as well as power/energy management strategy for a multi-unit system specifies the stress level of the converter components.

Reliability of power converters can be estimated by the reliability of its failure prone components. Classic reliability assessment methods, e.g., MIL-HDBK-217, models the failure rates considering different overestimated constants modeling the impact of environmental and operational condition without considering physical randomness, statistical and model uncertainties. However, mission profile-based approaches employ physics of failure techniques together with the uncertainty analysis in order to estimate the fragile components reliability. Therefore, considering the reliability behavior of key components and root causes of failure mechanisms, the converter reliability can be properly modeled.

Power electronic reliability engineering efforts aim at improving the reliability of power converters. The individual converter reliability can be enhanced by employing Design for Reliability (DfR) concepts [5]–[10] and various active control strategies [2], [6], [7], [11]–[16]. However, reliability improvement in a multi-converter system requires analyzing the system level impact of mission profiles and architectures on the reliability. The state-of-the-art reliability prediction methods estimate an individual converter lifetime to avoid or limit its components to a specific level of reliability. However, modern power systems consist of different converters with various applications and structures. Design, control, planning and operation of such systems require deep understanding the impact of mission profiles, control strategies, converter structures, and operating interactions among converters.

With the recent advances in power electronics, dc power systems, are gaining more interest over ac systems [17]–[20]. Therefore, this paper investigates the impact of mission profiles and system architecture on the reliability of multiple power converters operating in a dc microgrid. Reliability analysis in a dc microgrid based on wearing

This work was supported by the Reliable Power Electronic-Based Power System (REPEPS) project at the Department of Energy Technology, Aalborg University as a part of the Villum Investigator Program funded by the Villum Foundation.

This article has been accepted for publication in a future issue of this journal, but has not been fully edited. Content may change prior to final publication. Citation information: DOI 10.1109/TIA.2019.2920470, IEEE Transactions on Industry Applications

out of semiconductor devices studied in [21]. While, this paper presents a comprehensive reliability analysis considering the influence of semiconductor devices and capacitors. Furthermore, in order to point out the impact of mission profile, climate conditions of two locations and load profile of apartment and clinic loads with different characteristics are considered. In the following, the microgrid structure and its control strategy are explained in Section II. Afterwards, the converter reliability estimation approach is explained in Section III. Numerical analysis and results are reported in Section IV. Finally, Section V summarizes the outcomes.

## II. DC MICROGRID STRUCTURE

Fig. 1 shows a typical dc microgrid with different kinds of energy resources including a Photo-Voltaic (PV) array as a renewable source, a Battery Storage (BS) unit and a Fuel Cell Stack (FCS) as a dispatch-able source. In the following part, the electrical model of the energy resources, the corresponding energy conversion stage and control strategy are explained.

### A. Energy resources

The operating point of the dc/dc converters (i.e., duty cycle) and hence its reliability can be affected by the input voltage, which is specified by the energy resources. Thereby, the dynamic behavior of the input voltage of energy resources is accurately modeled as shown in Fig. 2. The PV array includes three parallel-connected strings, which have five series-connected panels. The output power-voltage characteristics of the PV array in terms of solar irradiance and ambient temperature are shown in Fig. 2(a) and the PV panel specifications are summarized in Table I. Furthermore, the output voltage-current characteristics of a Proton-exchange membrane 5 kW FCS is shown in Fig. 2(b) [22]. Moreover, a 1000Ah Lead-Acid battery storage is considered with the output voltage-current characteristics shown in Fig. 2(c) in terms of its State Of Charge (SOC) level.

### B. Converter topologies and control

The input voltage for the PV converter is between 250 V and 350 V as shown in Fig. 2(a), and hence a conventional boost converter can properly interface the PV array to a dc grid with a rated voltage of 400 V. The converter structure and the corresponding control block diagram are shown in Fig. 1(a). Furthermore, following Fig. 2(b) the FCS voltage is between 72 V and 110 V, and hence, a converter with a higher voltage gain and a higher input current is required. Therefore, a Four-phase Floating Interleaved Boost Converter (FFIBC) [23]–[25] as shown in Fig. 1(b) is considered for the FCS. The corresponding control block diagram is also shown in Fig. 1(b). The battery storage (BS) is connected to the dc grid through a bi-directional boost converter as shown in Fig. 1(c) illustrating the converter topology and its control block diagram. Furthermore, the converters parameters are summarized in Table II.

### C. FCS converter switching scheme

Suitable switching scheme by considering 90° phase shift between the carrier signal of each phase in the FFIBC can intensively reduce the input current ripple [24], [26], which can enhance the lifetime of the FCS. However, this paper proposes another switching scheme considering 90° phase shift between phases 1, 3, 2, and 4 (see Fig. 1(b)) respectively, which can reduce the ripple current of output capacitors as well. Applying 180° phase shift between phases 1 and 2 (and also between phases 3 and 4) can significantly reduce the output capacitor's current ripple and hence extend its lifetime.

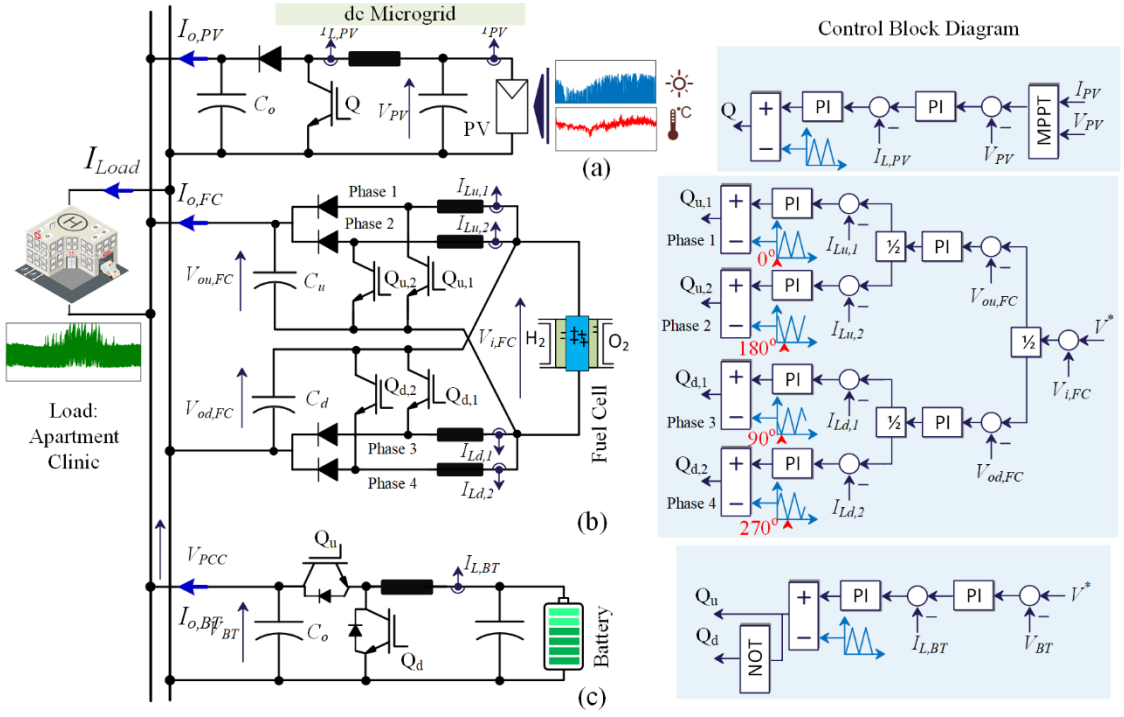


Fig. 1. Topology of the dc microgrid including their control structure.

This article has been accepted for publication in a future issue of this journal, but has not been fully edited. Content may change prior to final publication. Citation information: DOI 10.1109/TIA.2019.2920470, IEEE Transactions on Industry Applications

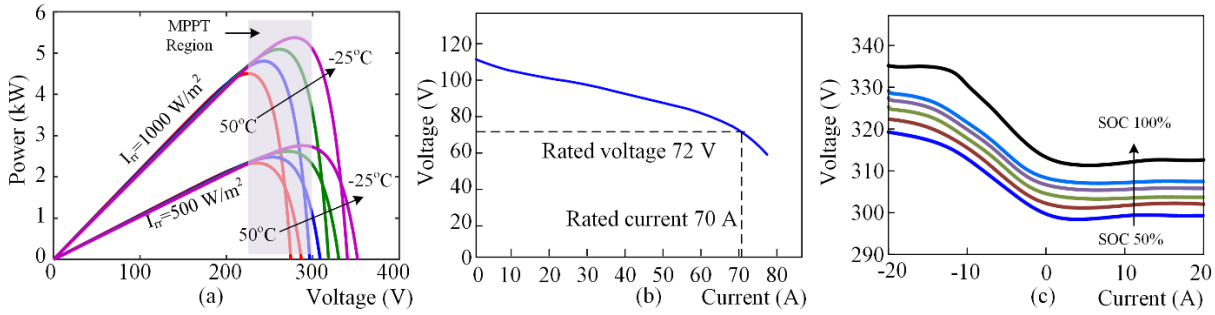


Fig. 2. Output characteristics of energy resources, (a) PV array, (b) Fuel Cell Stack (FCS), and (c) Battery Storage.

Table I. PV Panels and PV System parameters.

| Parameter | Symbol | Value |
|---|---|---|
| Panel Rated Power | $P_r$ (W) | 345 |
| Open Circuit Voltage | $V_{oc}$ (V) | 64.8 |
| Short Circuit Current | $I_{sc}$ (A) | 7.04 |
| MPPT Voltage | $V_m$ (V) | 54.7 |
| MPPT Current | $I_m$ (A) | 6.26 |
| Voltage temp. Coeff. | $\alpha$ (%/K) | -0.27 |
| Current temp. Coeff. | $\beta$ (%/K) | 0.05 |
| Number of Series panels | $N_s$ | 5 |
| Number of Parallel panels | $N_p$ | 3 |

Table II. Power converter parameters.

| Converter Parameters | PV converter | FCS Converter | Battery Converter |
|---|---|---|---|
| Rated power | 5 kW | 5 kW | 5 kW |
| Switching frequency | 20 kHz | 20 kHz | 20 kHz |
| Output capacitor | 2×200 µF ($C_o$) | 5×200 µF ($C_u$, $C_d$) | 2×200 µF ($C_o$) |
| ESR per capacitor @ 100 Hz | 0.35 Ω | 0.24 Ω | 0.35 Ω |
| Capacitor thermal resistance | 19.5 K/W | 28 K/W | 19.5 K/W |
| Capacitor thermal time constant | 10 min | 10 min | 10 min |
| DC inductor | 1 mH | 1 mH | 1 mH |
| IGBT | IGB15N60T | IGB15N60T | IGB15N60T |
| Diode | IDV20E65D1 | IDV20E65D1 | - |
| Battery capacity | | | 1000 Ah |

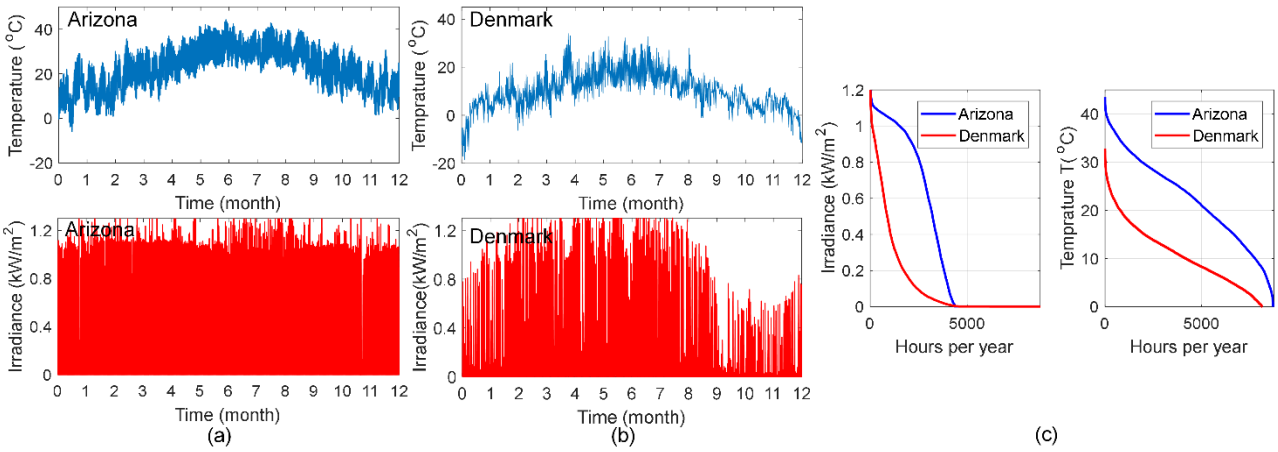


Fig. 3. Annual solar irradiance and ambient temperature for (a) Arizona, (b) Denmark. (c) Solar irradiance-duration, ambient temperature-duration and temperature swing-duration for Arizona and Denmark.

This article has been accepted for publication in a future issue of this journal, but has not been fully edited. Content may change prior to final publication. Citation information: DOI 10.1109/TIA.2019.2920470, IEEE Transactions on Industry Applications

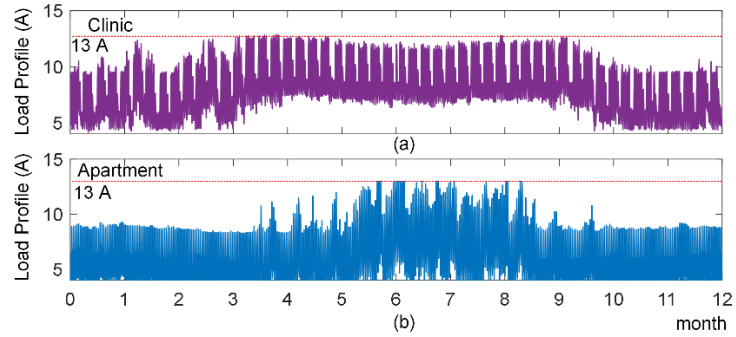


Fig. 4. Annual load demand for (a) small clinic and (b) apartment in the dc microgrid.

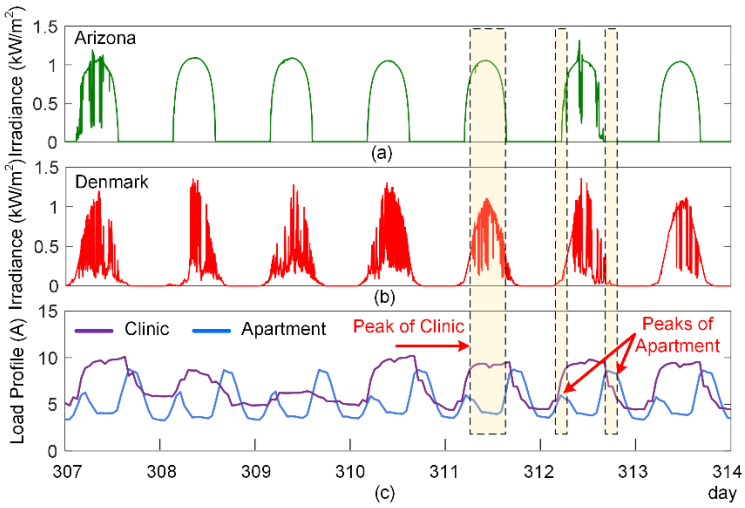


Fig. 5. Solar irradiance of (a) Arizona, (b) Denmark, and (c) load current of clinic and apartment during the days of 307 to 314.

### *D. Mission profiles*

The loading profile of the converters depends on the microgrid load profile and output power of renewable resources, which can be correlated by the energy management strategy provided in the dc microgrid. The PV system is considered as a renewable resource, and the annual solar irradiance on a tilt angle equal to the region latitude, and ambient temperature for two different regions, Arizona and Denmark, are shown in Fig. 3(a) and (b). Moreover, the annual irradiance and the annual temperature are shown in Fig. 3(c).

In order to model the load demand, two types of loads are considered including a small clinic and an apartment load as shown in Fig. 4(a) and (b). The reasons of selecting these types of loads are the differences in their annual peak load and its duration, daily peak load and its duration and occurrence time as well as the significance of the clinic load rather than the apartment load in terms of reliability. This is depicted in Fig. 4(a), which the annual peak load of the clinic is almost 6 months, while it is only about 3 months for the apartment load. Notably, the generation and storage systems are designed for the peak load of 13 A for both cases. These differences may affect the annual load profile of the converters, and consequently, their aging process. Moreover, the daily load profile and solar irradiance for 307$^{th}$ to 314$^{th}$ days of a year are shown in Fig. 5. It can be seen that the daily peak of the clinic is concurrent with the solar irradiance. However, the peak load of the apartment happens in the morning and in the evening when the solar power is not available. This fact may affect the loading profile of the battery storage and consequently the FCS converters.

### *E. Energy management system*

Energy management system controls the energy and power flow within the microgrid in order to supply its demand by extracting the maximum allowable power from PV array and taking into account the energy storage level of battery, SOC. The PV system is operating in the MPPT mode under different climate conditions, i.e., solar irradiance and ambient temperature, to supply the load and charge the battery if the SOC is lower than 100%. If the PV and battery cannot support the load, the FCS has to supply the remaining power of the system. Notably, the battery storage is only charged by the PV power (renewable energy). In order to enhance the lifetime of the battery, the maximum depth of discharge of 50% is recommend in the energy management system [27], [28]. The power flow among different energy sources during a day is shown in Fig. 6 indicating different loading profiles for PV, battery and FCS according to the load profile and SOC of BS. The annual load energy, converted energy by PV, FCS converters and absolute converted energy by the battery converter are reported in Table III.

## III. Converter Reliability Estimation

Active switches and capacitors are two of the most fragile components widely concerned in power electronic converters [3]. These components should be appropriately designed at a desired strength level in order to withstand

This article has been accepted for publication in a future issue of this journal, but has not been fully edited. Content may change prior to final publication. Citation information: DOI 10.1109/TIA.2019.2920470, IEEE Transactions on Industry Applications

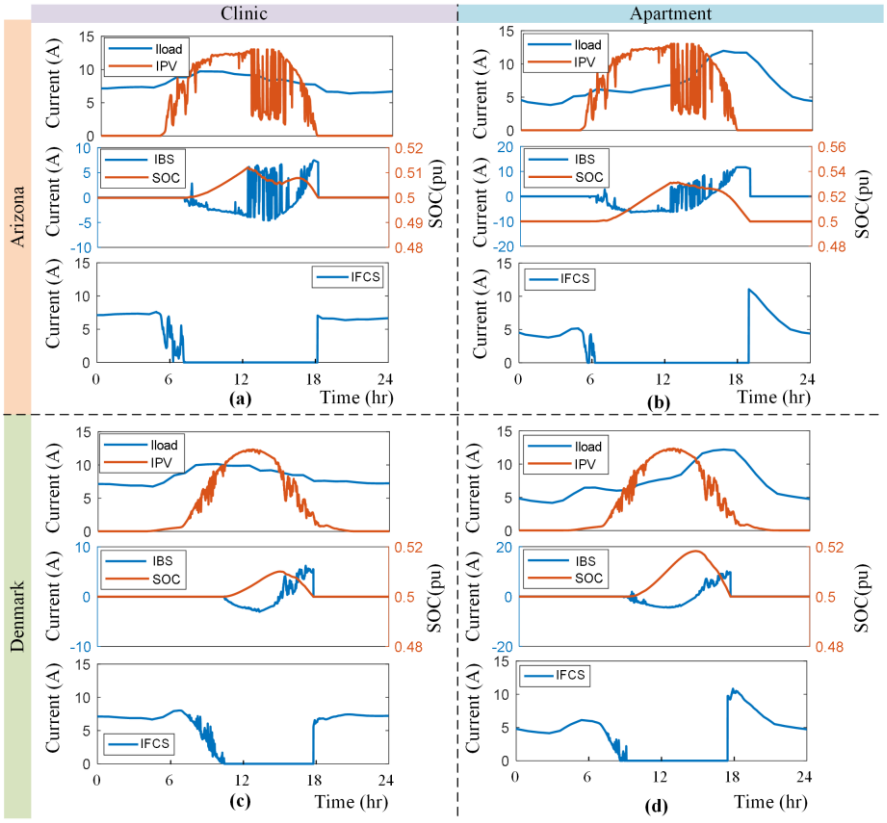


Fig. 6. Power sharing among different energy units in (a) Case I: Arizona-clinic load, (b) Case II: Arizona-Apartment load, (c) Case III: Denmark-Clinic load, and (d) Case IV: Denmark-Apartment load – IBS: Battery Storage Current, IFCS: Fuel Cell Stack Current, IPV: PV current, Iload: load Current.

Table III. Annual converted Energy by the power converters for different Cases in the dc microgrid.

| Case | Region | Load Type | Load Energy (MWh/yr) | FC Energy (MWh/yr) | PV Energy (MWh/yr) | Absolute Battery Energy (MWh/yr) |
|---|---|---|---|---|---|---|
| I | Arizona | Clinic | 28.813 | 12.866 | 15.747 | 4.632 |
| II | | Apartment | 20.570 | 4.736 | 15.634 | 15.050 |
| III | Denmark | Clinic | 28.813 | 22.586 | 6.064 | 0.918 |
| IV | | Apartment | 20.570 | 14.357 | 6.051 | 3.409 |

applied stresses – such as the electrical loading and thermal cycling – during a target lifetime. The designed strength and applied stress have a range of distribution due to the manufacturing, operational and model uncertainties condition variations, and hence, the probability of failure can be estimated from the mismatch of stress and strength levels on each device. In this paper, the failure probability of the converter components will be estimated employing the mission profile based reliability approach discussed in [29].

The main failure stressors on power electronic converters are typically caused by electrical loading and temperature cycling. These stress sources should be translated into thermal stresses on the devices. Afterwards, the components failure probability and reliability can be estimated employing either experimental models or Monte-Carlo simulations. In this study, an experimental model [29] is used for estimating the capacitor lifetime. Furthermore, the reliability of active switches is estimated by applying Monte-Carlo simulations and an empirical lifetime model.

### *A. Electro-thermal stress mapping*

State-of-the-art lifetime models of a device are based on the thermo-mechanical behavior of its materials. Therefore, the electrical loading of a device should be translated into a thermal stress such as hot-spot or junction temperature. The electro-thermal models of capacitor, diode, and IGBT are shown in Fig. 7(a), (b) and (c) respectively. In this study, the Foster model is employed as it is given in the component's datasheet. Furthermore, the heatsink temperature is assumed to be constant and 20°C higher than the ambient temperature.

In order to carry out the electro-thermal stress mapping, each converter is simulated individually under different loading conditions and ambient temperature. Afterwards, the hot-spot temperature of capacitor, $T_h$, junction temperature of diode, $T_{j\text{-}D}$ and junction temperature of IGBT, $T_{j\text{-}Q}$ are summarized in a look-up tables as shown in Fig. 7(d). In the next step, power flow program is employed to find out the annual loading profile of converters ($I_{CL}$) according to the energy management strategy and mission profiles ($I_{rr}$, $T_a$, $I_{Load}$) as shown in Fig. 8(a). Therefore, the annual profile of capacitor hot-spot temperature, diode and IGBT junction temperatures are found by employing the look-up tables established for each converter. These temperatures are utilized to predict the reliability of the components as explained in the following.

This article has been accepted for publication in a future issue of this journal, but has not been fully edited. Content may change prior to final publication. Citation information: DOI 10.1109/TIA.2019.2920470, IEEE Transactions on Industry Applications

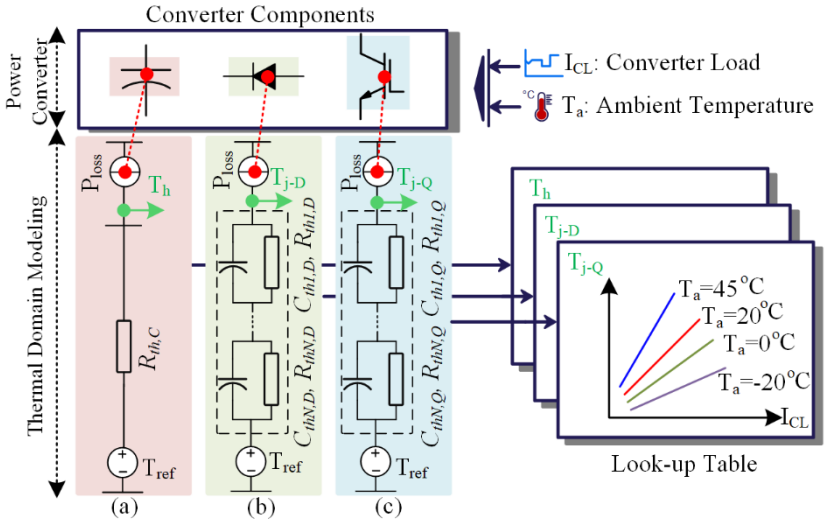


Fig. 7. Electro-thermal modelling of a converter; (a) capacitor, (b) diode, (c) IGBT.

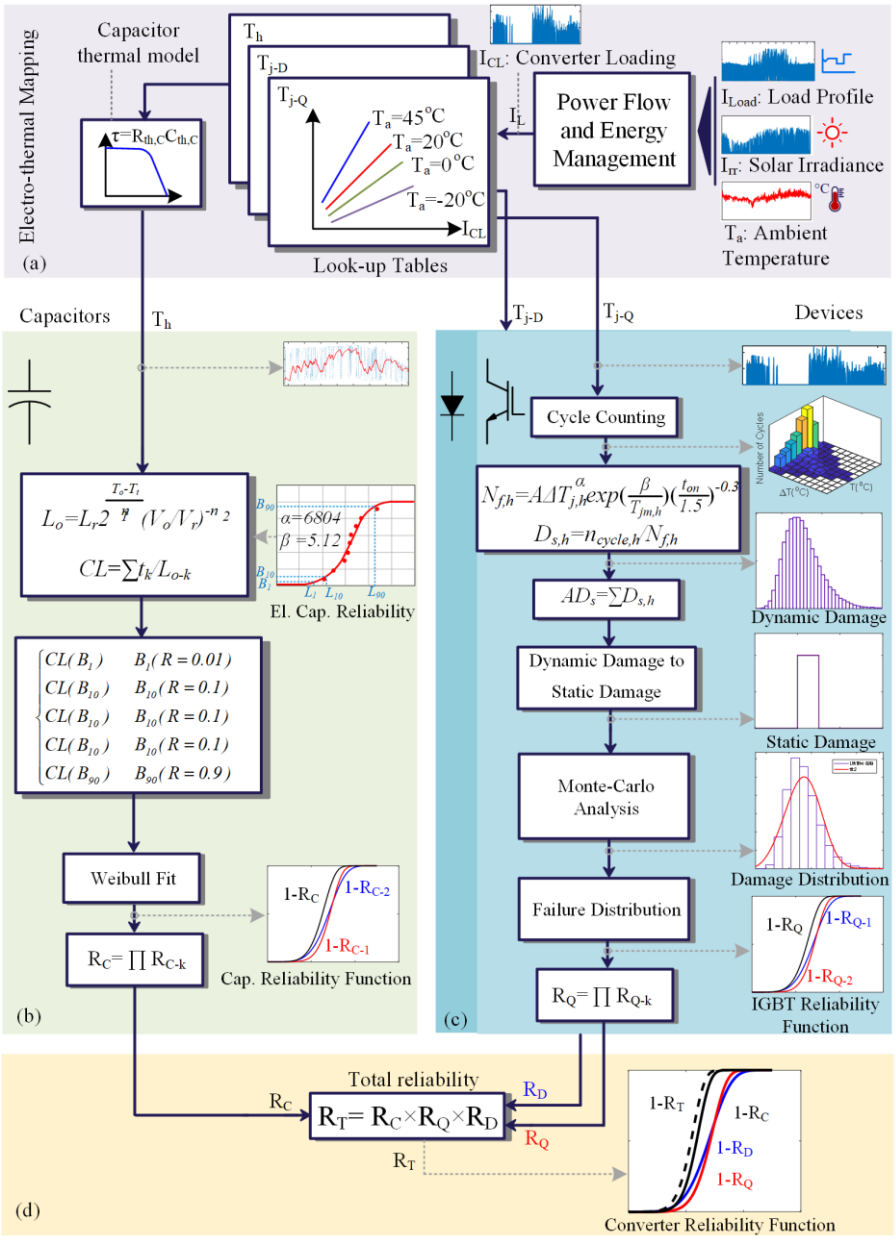


Fig. 8. Reliability estimation procedure of a power converter: (a) electrolytic capacitors, (b) active switches (Diode and IGBT).

This article has been accepted for publication in a future issue of this journal, but has not been fully edited. Content may change prior to final publication. Citation information: DOI 10.1109/TIA.2019.2920470, IEEE Transactions on Industry Applications

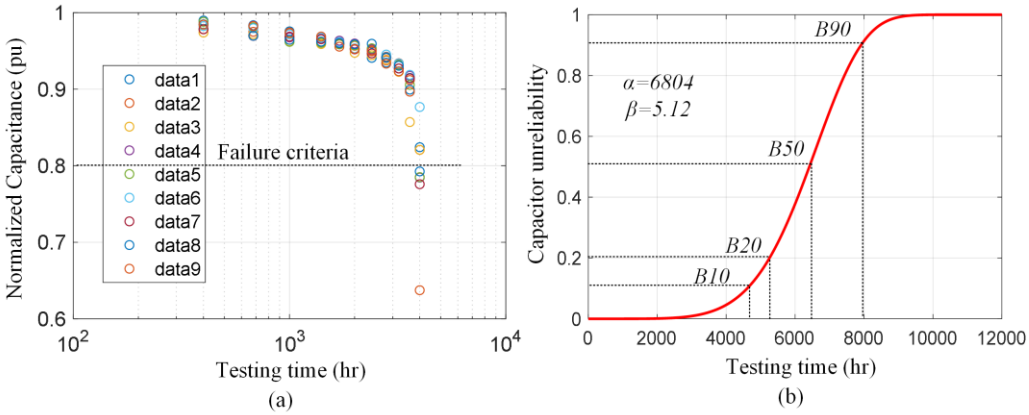


Fig. 9. Capacitor degradation testing results at rated voltage, rated ripple current and upper category temperature (105 ºC). (a) Normalized capacitance; (b) Capacitor time to failure distribution function [29].

### *B. Capacitor reliability modeling*

According to [30], [31], the lifetime model of electrolytic capacitors depends on the operating voltage and hot-spot temperature as:

$$L_o = L_r \cdot 2^{\frac{T_r - T_o}{n_1}} \cdot \left(\frac{V_o}{V_r}\right)^{-n_2}, \quad (1)$$

where $L_r$ and $L_o$ are the lifetime under rated and operating conditions, $T_r$, $T_o$ are the rated and operating hot-spot temperatures, and $V_r$, $V_o$ are the rated and operating voltages. The constant exponents of $n_1$ and $n_2$ can be obtained from [31], which in this paper are $n_1$ = 10 and $n_2$ = 4.2. The consumed lifetime ($CL$) of an individual capacitor during a year is expressed as:

$$CL = \sum_{k=1}^{N} \frac{t_k}{L_{o-k}} = \sum_{k=1}^{N} \frac{t_k}{L_r \cdot 2^{\frac{T_r - T_{o-k}}{n_1}} \cdot \left(\frac{V_{o-k}}{V_r}\right)^{-n_2}} \quad (2)$$

where $t_k$ is the duration of operation under the operating temperature, $T_{o\text{-}k}$, and voltage $V_{o\text{-}k}$ is the $k^{th}$ sample of the mission profile. The reciprocal of $CL$ presents the lifetime of the capacitor under a given mission profile. In order to obtain the failure density function, several capacitors can be tested applying a target mission profile. This procedure is time consuming and the reliability data cannot be applied for other mission profiles, and therefore, the lifetime estimation can be performed by testing some capacitors under a rated voltage, a ripple current and an upper category temperature. These results can be used for estimating the failure density function of similar capacitors with a same technology, rated lifetime, and upper category temperature.

For instance, in this study, the reliability test data for an electrolytic capacitor (56 µF, 35 V) with a rated lifetime of 5.000 hr and an upper category temperature of 105 ºC provided by [29] are employed. In this test, nine capacitors were tested and the normalized capacitance of them are summarized in Fig. 9(a). The end of life criterion of the individual capacitor is when its capacitance drops by 20% to its initial value. The failure probability distribution function for these test results are shown in Fig. 9(b) which is fitted by the Weibull distribution function with a 50% confidence level [29] as:

$$Q(t) = 1 - \exp\left(-\left(\frac{t}{\alpha}\right)^{\beta}\right) \quad (3)$$

where $\alpha$ and $\beta$ are the scale and shape factors. The shape factor $\beta$ depends on the failure mechanisms and material characteristics of capacitors and it is not affected by the operating condition. Hence, for different mission profiles, the capacitors with a same materials will have a same shape factor equal to 5.12 [29]. However, the scale factor depends on the operating condition and it is equal to a time when the accumulated failure probability distribution reaches 0.63. In order to estimate $\alpha$ by employing test data for a desired mission profile, the $B_x$ lifetime can be calculated by the reciprocal of $CL$ in (2) for different $B_x$ rated lifetime $L_r$ provided in Fig. 9(b). Thereafter, the $B_x$ lifetime data is fitted by the Weibull distribution function to find out $\alpha$ and $\beta$, where $\beta$ is equal to 5.12 as mentioned before. Therefore, the capacitor unreliability function can be expressed by the Weibull distribution function with the calculated $\alpha$ and $\beta$. Finally, it is assumed that the converter malfunctions if one of the capacitors fails. Therefore, the reliability of the capacitor bank can be obtained by a series reliability network model as:

$$R_C = \prod_{k=1}^{N_C} R_{C-k} \quad (4)$$

in which $R_C$ being the reliability of capacitor bank, $R_{C\text{-}k}$ is the reliability of individual capacitor, and $N_C$ is the number of capacitors. The capacitor reliability calculation procedure is illustrated in Fig. 8(b).

### *C. Power semiconductor switches reliability modeling*

The main dominant failure mechanisms on the power switches are solder joint fatigue and bond-wire cracking/lift off. The number of cycles to failure ($N_{fs}$) due to the solder joint failure is related to the case temperature variation $\Delta T_c$ which can be calculate by (5), where $K$ and $\gamma$ being the curve fitting parameters.

$$N_{fs} = K \cdot \Delta T_c^{\gamma} \quad (5)$$

Furthermore, following power cycling tests provided in [32], the lifetime of semiconductor switches, IGBT and diode, depends on a minimum (/or mean) junction temperature, temperature swing and its heating time. The empirical lifetime model presented in [32] illustrates the number of cycles to failure, $N_f$, as:

$$N_f = A \cdot (\Delta T_j)^{-\beta_1} \cdot \exp\left(\frac{\beta_2}{T_{j,\min} + 273}\right) \cdot t_{on}^{\beta_3} \quad (6)$$

This article has been accepted for publication in a future issue of this journal, but has not been fully edited. Content may change prior to final publication. Citation information: DOI 10.1109/TIA.2019.2920470, IEEE Transactions on Industry Applications

where $T_{j,min}$ is the minimum junction temperature, $\Delta T_j$ is the junction temperature swing, $t_{on}$ is the heating time of the power cycling. Moreover, the constants $A$, $\beta_1$ , $\beta_2$, and $\beta_3$ can be obtained according to test data provided in [32]. Furthermore, power cycles with a heating time below 60 seconds highly contribute to the bond wire wear out, hence, the number of cycles to failure for different $t_{on}$ is modeled as [33]:

$$\frac{N_f(t_{on})}{N_f(1.5)} = \begin{cases} 2.25, & t_{on} \le 0.1s \\ \left(\frac{t_{on}}{1.5}\right)^{-0.3}, & 0.1s \le t_{on} \le 60s \\ 0.33, & t_{on} \ge 60s \end{cases} \quad (7)$$

Following Fig. 8(c), the annual junction temperature of IGBT and diode should be decomposed and classified by a cycle counting methods, for example using the rain-flow algorithm, into $h$ classes in order to obtain the number of cycles of $N_h$, minimum temperature, $T_{j,min-h}$, temperature swing $\Delta T_{j-h}$ and heating time $t_{on-h}$ for $h^{th}$ class. The number of cycles to failure for class $h$, $N_{f-h}$, is found by substituting $T_{j,min-h}$, $\Delta T_{j-h}$ and $t_{on-h}$ into (6) and (7). Therefore, the damage of class $h$, $D_h$, on the device is calculated by:

$$D_h = \frac{N_h}{N_{f-h}} . \quad (8)$$

Consequently, according to the Miner's rule, the annual accumulated damage ($AD$) linearly depends on the individual damage of each temperature cycle and can be expressed as $AD = \sum D_h$. Following [4], the accumulated damage, heating time, number of cycles and minimum and swing temperature values should be translated into static values with the same damage effect on the device. The reciprocal of this accumulated damage presents the lifetime of the device. However, in practice, the lifetime model parameters as well as the device electrical and thermal parameters are not constant and should have a distribution due to the manufacturing, operational and model uncertainties. In this study, 90% confidence level for model parameters $A$, $\beta_1$, $\beta_2$, and $\beta_3$ and operating parameters $T_{j,min}$, $\Delta T_j$ , and $t_{on}$ are considered in order to obtain the lifetime of each devices. Afterwards, a population of 10,000 power switches is employed in Monte-Carlo simulation in order to obtain the failure density function, and cumulative distribution function, also called unreliability function, for each device. Finally, the converter failure occurs if one of the switches fails. Hence, according to series reliability network modeling, the reliability of IGBTs and diodes can be obtained by multiplying the reliability of individual device as:

$$R_Q = \prod_{k=1}^{N_Q} R_{Q-k}, \quad R_D = \prod_{k=1}^{N_D} R_{D-k} \quad (9)$$

where $R_Q$ and $R_D$ are the reliability of IGBT and Diode, $N_Q$ and $N_D$ are the number of IGBTs and diodes of the converter.

### D. Converter reliability calculation

The converter reliability depends on the reliability of each components, and any component (e.g., diode, and/or IGBT, and/or capacitor) malfunction causes converter failure. Hence, following reliability network model, the converter reliability is defined as a series connection of individual components as. Therefore, the total converter reliability ($R_T$) is equal to:

$$R_T = R_C \times R_Q \times R_D . \quad (10)$$

Notably, the unreliability function is the complementary of $R_T$. The predicted unreliability function in this paper is attributed to the accumulated failure probability due to the wear out of converter hardware, i.e, its fragile components, while other failure sources such as random failures and software malfunction are not considered in this paper.

## IV. Reliability Estimation – Numerical Analysis

In this section, the accumulated probability of the converters due to the wear out of IGBTs, diodes and capacitors, here called unreliability, is shown in Fig. 1. Converters wear out probability is estimated under mission profiles of Arizona and Denmark with the load profiles of a small clinic and an apartment. The obtained results are discussed in the following. Moreover, the impact of switching scheme on the FCS reliability is explained subsequently.

### A. Impact of mission profiles

***Impact of environmental conditions – 1:*** According to Fig. 10, the very first observation that can be made is that the converters operating in Denmark are more reliable than in Arizona as shown in Fig. 10 for both types of loads. This is due to the higher solar energy potential in Arizona as shown in Fig. 3, which directly affects the loading of PV converters. Furthermore, it induces more power cycles to the other converters and consequently reducing their reliability as well. Moreover, the high ambient temperature in Arizona increases the thermal damages of the converters' components. Therefore, the climate condition affects the reliability of converters operating in a microgrid and it must be taken into account during design and planning procedure.

***Impact of environmental conditions – 2:*** The output capacitor banks have a dominant impact on the reliability of the battery and FCS converters. However, in Denmark, the PV converter reliability is limited by the active switches, such as IGBTs and afterwards, diodes, while for the PV converter in Arizona, the capacitor bank still has the dominant influence. In order to investigate the reason behind this behavior, the annual accumulated damage on the IGBT, diode and capacitor bank of the PV converter under given mission profiles are reported in Fig. 11(a). As it can be seen, the damage of the capacitor bank is almost ten times the IGBT in Arizona, while the IGBT and Diode damages are negligible. However, in Denmark, the capacitor bank damage is small and comparable with the IGBT and diode damages. This is due to the fact that the annual converted power by PV, and consequently, the loading of the capacitor bank in Denmark is lower than in Arizona according to Fig. 3 and Table III. Meanwhile, the PV converter has encountered more power cycles (current swings) under Denmark mission profile than Arizona as shown in Fig. 11(b). Hence, the IGBT and diode damages in the case of the Denmark mission profile is high. Therefore, the active switches have a significant impact on the PV converter reliability in Denmark, while the capacitor

This article has been accepted for publication in a future issue of this journal, but has not been fully edited. Content may change prior to final publication. Citation information: DOI 10.1109/TIA.2019.2920470, IEEE Transactions on Industry Applications

bank is limiting its reliability in Arizona. Moreover, according to Fig. 11(a), the total damage of the PV converter under the Denmark mission profile is quite lower than its damage under Arizona mission profile, implying a better reliability for the PV converter in Denmark rather than in Arizona as shown in Fig. 10.

***Impact of operational conditions – 1:*** The reliability of the battery converter in clinic load is better than the apartment load as shown in Fig. 10. Following Fig. 5 and Fig. 6, the peak of the clinic load occurs concurrent with the sunny hours, while the peak of the apartment load happens in the morning and evening when there is no solar power. Hence, following the energy management strategy, the loading of the battery converter in the case of apartment is higher than in the clinic as reported in Table III. This fact is due to the daily peak load characteristics, and it can be improved by demand side management or peak shaving if it is possible.

***Impact of operational conditions – 2:*** Furthermore, the FCS converter reliability in clinic load is less than the apartment load as shown in Fig. 10. According to the energy management strategy, the FCS converter has to supply the mismatch energy between the PV and the load. Comparing the annual load profiles shown in Fig. 4, the annual peak load duration in the clinic is almost 6 months, while it is 3 months for apartment. Furthermore, the annual energy of clinic load is 1.4 times of the apartment load as reported in Table III. Considering the same rating for FCS converter, which is sized based on annual peak load of 13 A, its higher loading in clinic load reduces corresponding reliability.

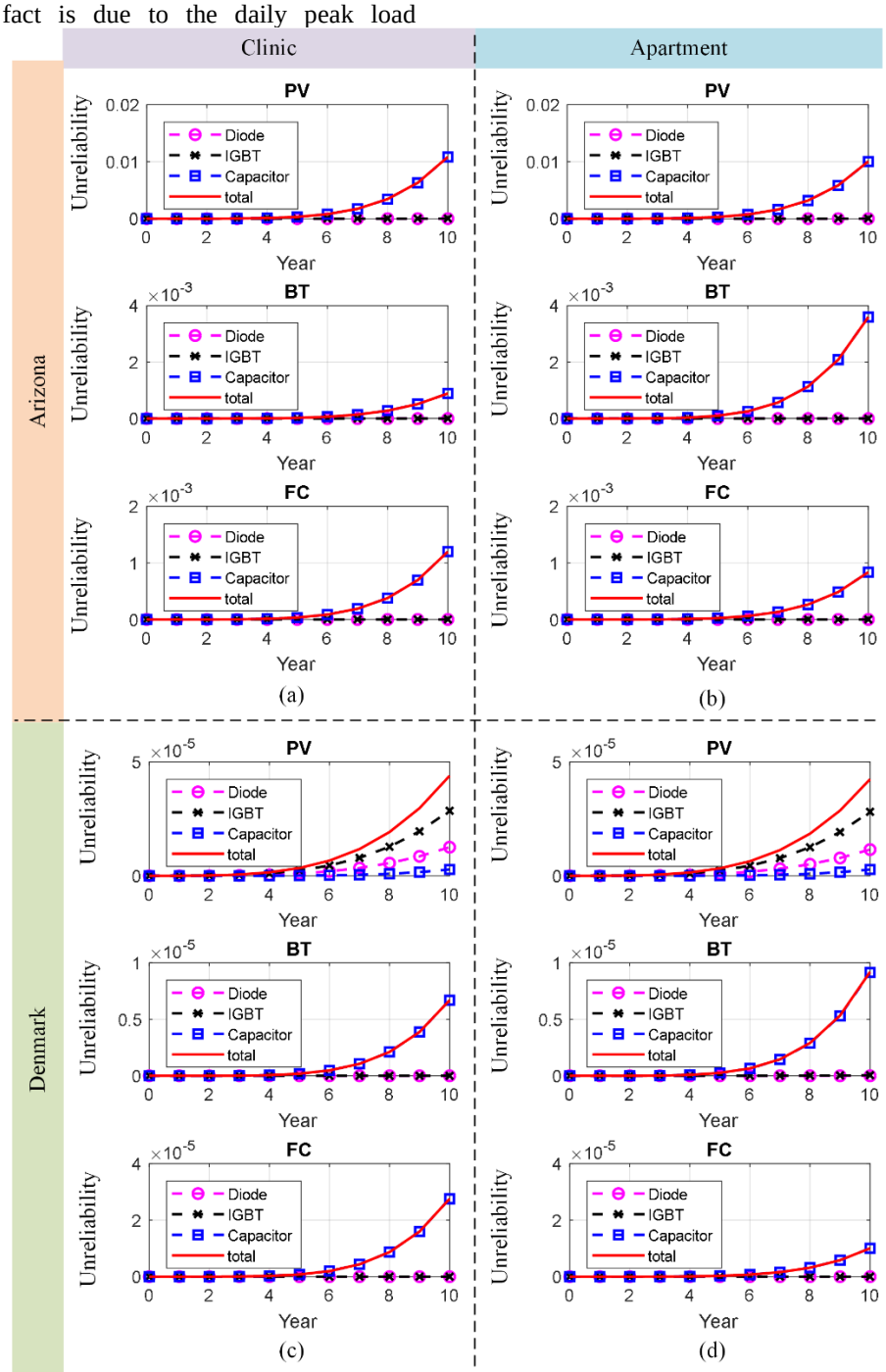


Fig. 10. Accumulated failure probability of converters due to the wear out of IGBTs, diodes, and capacitors function of converters within their useful lifetime; (a) Case I: Clinic load in Arizona, (b) Case II: Apartment load in Arizona, (c) Case III: Clinic load in Denmark, (d) Case IV: Apartment load in Denmark – PV: Photo-Voltaic, BT: Battery, FC: Fuel Cell.

This article has been accepted for publication in a future issue of this journal, but has not been fully edited. Content may change prior to final publication. Citation information: DOI 10.1109/TIA.2019.2920470, IEEE Transactions on Industry Applications

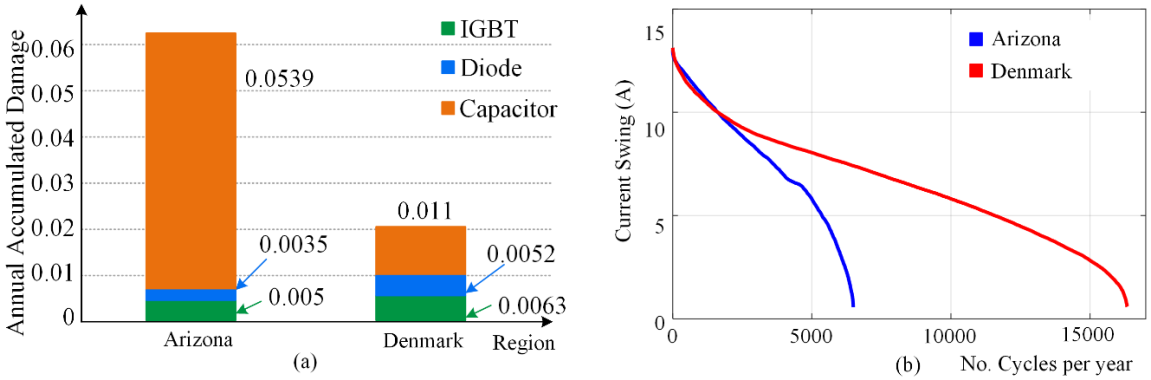


Fig. 11. PV converter damage analysis; (a) Annual damage on the converter components and (b) power cycling (current swing) on the converter under mission profiles of Arizona and Denmark.

### B. *Impact of system architecture*

***Impact of energy resources:*** As already mentioned, the system architecture is one of the affecting factors on the converter reliability. In this study a dc microgrid with one dispatchable unit, FCS, one non-dispatchable unit, PV and storage system is considered as shown in Fig. 1. Therefore, three different kinds of energy resources are employed. According to the energy management system, the PV converter is operated in MPPT mode, and hence it experiences any stresses induced by PV arrays. However, the FCS and battery are almost constant DC sources; hence, the thermal stress on these converters comes from PV and load. Even though the FCS converter has more components, the PV converter has the least reliability. Therefore, this clearly highlights the converter reliability dependency on the energy resources.

***Impact of application (load):*** Furthermore, utilizing of the considered DC microgrid for a clinic application has different reliability characteristics compared to an apartment application. As shown in Fig. 10, the battery converter reliability in clinic load is better than apartment load. Meanwhile, the FCS converter has higher reliability in apartment load application. However, the reliability of battery and FCS converters in Arizona is almost 0.999. As the clinic is a very sensitive load, the reliability of these converters should be redesigned to enhance its reliability. Moreover, the PV converter reliability may be not acceptable for clinic application in Arizona, where it is 0.99 within a 10-year operation. Therefore, application-specific analysis identifies the weakest converters in the system level, which should be improved to reach a desired level of reliability.

### C. *Impact of control level*

***Impact of switching scheme on FCS converter reliability***: As already discussed, employing the proposed switching scheme can decrease the capacitor ripple currents in FCS converter FFIBC. The current waveform of inductors and the up-stage (phase 1 and 2) capacitor bank of the FFIBC, with the regular and proposed switching schemes are shown in Fig. 13 at a full load condition. As a result, the RMS value of the capacitor ripple current at full load condition can be decreased by 15% and consequently improving the reliability of the capacitors and the converter. For instance, the reliability of the FCS converter under regular and proposed switching scheme supplying the clinic load in both regions is shown in Fig. 12 implying a notable enhancement of the overall converter reliability. As it can be seen from Fig. 12, employing the proposed switching scheme will decrease the FCS converter unreliability from 6.6E-3 to 1.2E-3 for the Arizona mission profile and from 4E-3 to 3E-5 for the Denmark mission profile.

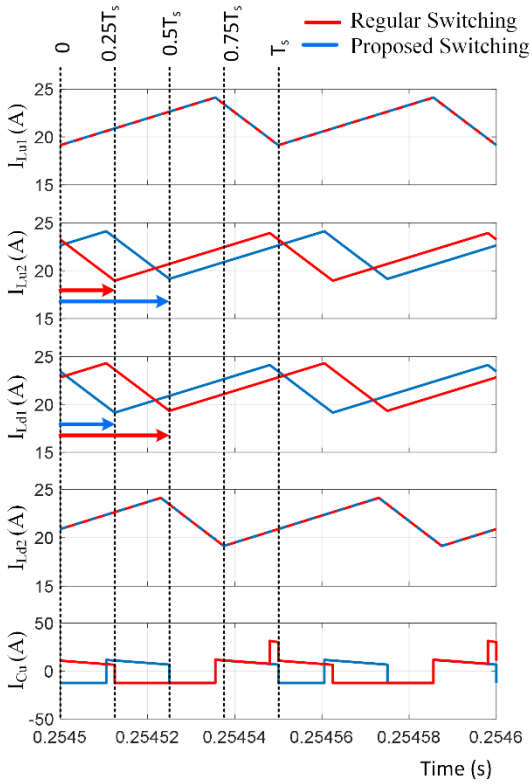


Fig. 13. Effect of switching pattern in the capacitor ripple current.

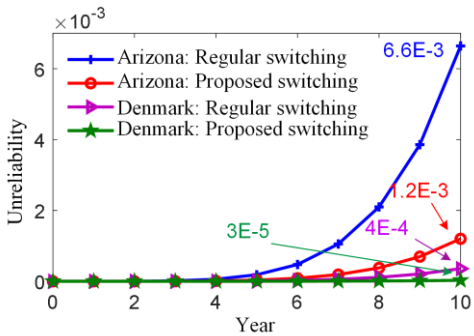


Fig. 12. Unreliability of FCS converter under different switching schemes suppling the clinic load.

## V. Conclusion

This paper has explored the impact of mission profile, control strategy, and operation interaction among multiple connected converters with different applications. As a result, it provides deeper system-level insight into design, operation and planning of modern power systems for reliability assessment and risk management.

According to the analysis, mission profiles have the significant impact on the power converter reliability. For instance, the PV converter unreliability in Arizona is almost 200 times of that in Denmark. Furthermore, the load profile characteristics affects the loading and consequently the reliability of the converters. As an example, the battery converter unreliability under apartment load is almost 2~3 times of that under the clinic load.

Another factor affecting the converter reliability is its application and topology. The PV converter has the lowest reliability since it experiences the whole solar irradiance and ambient temperature fluctuations. While the thermal stress induced by PV power and load profile is shared between the battery and fuel cell converters. According to the analysis, under given operating conditions, the PV converter unreliability is almost 2~10 times of other converters.

Furthermore, depending on the application and mission profiles, different components may play a major role on the converter lifetime. The obtained results show that the PV converter reliability in Arizona is limited by the capacitors while the semiconductor devices have the dominant impact on its reliability in Denmark.

## References


[1] B. M. Ayyub and R. H. McCuen, "*Probability, Statistics, and Reliability for Engineers and Scientists*," 3rd ed. Taylor & Francis Group, 2015.

[2] Y. Song and B. Wang, "Survey on Reliability of Power Electronic Systems," *IEEE Trans. Power Electron.*, vol. 28, no. 1, pp. 591–604, Jan. 2013.

[3] J. Falck, C. Felgemacher, A. Rojko, M. Liserre, and P. Zacharias, "Reliability of Power Electronic Systems: An Industry Perspective," *IEEE Ind. Electron. Mag.*, vol. 12, no. 2, pp. 24–35, Jun. 2018.

[4] P. D. Reigosa, H. Wang, Y. Yang, and F. Blaabjerg, "Prediction of Bond Wire Fatigue of IGBTs in a PV Inverter under a Long-Term Operation," *IEEE Trans. Power Electron.*, vol. 31, no. 10, pp. 3052–3059, Mar. 2016.

[5] A. Isidori, F. M. Rossi, and F. Blaabjerg, "Thermal Loading and Reliability of 10 MW Multilevel Wind Power Converter at Different Wind Roughness Classes," in *Proc. IEEE ECCE*, 2012, pp. 2172–2179.

[6] Z. Qin, M. Liserre, F. Blaabjerg, and H. Wang, "Energy Storage System by Means of Improved Thermal Performance of a 3 MW Grid Side Wind Power Converter," in *Proc. IEEE IECON*, 2013, pp. 736–742.

[7] Y. Wu, M. A. Shafi, A. M. Knight, and R. A. McMahon, "Comparison of the Effects of Continuous and Discontinuous PWM Schemes on Power Losses of Voltage-Sourced Inverters for Induction Motor Drives," *IEEE Trans. Power Electron.*, vol. 26, no. 1, pp. 182–191, Jan. 2011.

[8] H. Wang, K. Ma, and F. Blaabjerg, "Design for Reliability of Power Electronic Systems," *IECON 2012 - 38th Annu. Conf. IEEE Ind. Electron. Soc.*, pp. 33–44, Oct. 2012.

[9] S. Peyghami, P. Davari, H. Wang, and F. Blaabjerg, "The Impact of Topology and Mission Profile on the Reliability of Boost-Type Converters in PV Applications," in *Proc. IEEE COMPEL*, 2018, pp. 1–8.

[10] S. Peyghami, P. Davari, H. Wang, and F. Blaabjerg, "System-Level Reliability Enhancement of DC/DC Stage in a Single-Phase PV Inverter," *Microelectron. Reliab.*, vol. 88–90, pp. 1030–1035, Sep. 2018.

[11] K. Ma, M. Liserre, and F. Blaabjerg, "Reactive Power Influence on the Thermal Cycling of Multi-MW Wind Power Inverter," *IEEE Trans. Ind. Appl.*, vol. 49, no. 2, pp. 922–930, Mar. 2013.

[12] H. Wang, A. M. Khambadkone, and X. Yu, "Control of Parallel Connected Power Converters for Low Voltage Microgrid—Part II: Dynamic Electrothermal Modeling," *IEEE Trans. Power Electron.*, vol. 25, no. 12, pp. 2971–2980, 2010.

[13] M. Andresen, G. Buticchi, and M. Liserre, "Study of Reliability-Efficiency Tradeoff of Active Thermal Control for Power Electronic Systems," *Microelectron. Reliab.*, vol. 58, pp. 119–125, Mar. 2016.

[14] C. J. J. Joseph, M. R. Zolghadri, A. Homaifar, F. Lee, and R. D. D. Lorenz, "A Novel Thermal Based Current Sharing Control of Parallel Converters," *2004 10th Int. Work. Comput. Electron. (IEEE Cat. No.04EX915)*, pp. 647–653.

[15] S. Peyghami, P. Davari, and F. Blaabjerg, "System-Level Reliability-Oriented Power Sharing Strategy for DC Power Systems," *IEEE Trans. Ind. Appl.*, DOI: 10.1109/TIA.2019.2918049, pp. 1–11, 2019.

[16] K. Ma and F. Blaabjerg, "Modulation Methods for Neutral-Point-Clamped Wind Power Converter Achieving Loss and Thermal Redistribution Under Low-Voltage Ride-Through," *IEEE Trans. Ind. Electron.*, vol. 61, no. 2, pp. 835–845, Feb. 2014.

[17] J. G. Ciezki and R. W. Ashton, "Selection and Stability Issues Associated with a Navy Shipboard DC Zonal Electric Distribution System," *IEEE Trans. Power Deliv.*, vol. 15, no. 2, pp. 665–669, Apr. 2000.

[18] D. Boroyevich, I. Cvetkovic, R. Burgos, and D. Dong, "Intergrid: A Future Electronic Energy Network?," *IEEE J. Emerg. Sel. Top. Power Electron.*, vol. 1, no. 3, pp. 127–138, 2013.

[19] P. Kou, D. Liang, J. Wang, and L. Gao, "Stable and Optimal Load Sharing of Multiple PMSGs in an Islanded DC Microgrid," *IEEE Trans. Energy Convers.*, vol. 33, no. 1, pp. 260–271, Mar. 2018.

[20] M. R. Hossain and H. L. Ginn, "Real-Time Distributed Coordination of Power Electronic Converters in a DC Shipboard Distribution System," *IEEE Trans. Energy Convers.*, vol. 32, no. 2, pp. 770–778, Jun. 2017.

[21] S. Peyghami, H. Wang, P. Davari, and F. Blaabjerg, "Mission Profile Based Power Converter Reliability Analysis in a DC Power Electronic Based Power System," in *Proc. IEEE ECCE*, 2018, pp. 1–7.

[22] "5000W Fuel Cell Stack User Manual," 2013. [Online]. Available: http://www.fuelcellstore.com/manuals/horizon-pem-fuel-cell-h-5000-manual.pdf. [Accessed: 24-Apr-2018].

[23] M. Kabalo, D. Paire, B. Blunier, D. Bouquain, M. G. Simoes, and A. Miraoui, "Experimental Validation of High-Voltage-Ratio Low-Input-Current-Ripple Converters for Hybrid Fuel Cell Supercapacitor Systems," *IEEE Trans. Veh. Technol.*, vol. 61, no. 8, pp. 3430–3440, Oct. 2012.

[24] M. Kabalo, D. Paire, D. Bouquain, B. Blunier, M. Godoy Simões, and A. Miraoui, "Experimental Evaluation of Four-Phase Floating Interleaved Boost Converter Design and Control for Fuel Cell Applications," *IET Power Electron.*, vol. 6, no. 2, pp. 215–226, Feb. 2013.

[25] A. Kolli, A. Gaillard, A. De Bernardinis, O. Bethoux, D. Hissel, and Z. Khatir, "A Review on DC/DC Converter Architectures for Power Fuel Cell Applications," *Energy Convers. Manag.*, vol. 105, pp. 716–730, Nov. 2015.

[26] C. D. Lute, M. G. Simoes, D. I. Brandao, A. Al Durra, and S. M. Muyeen, "Development of a Four Phase Floating Interleaved Boost Converter for Photovoltaic Systems," in *2014 IEEE Energy Conversion Congress and Exposition (ECCE)*, 2014, pp. 1895–1902.

[27] IEA Task III, "Lead-Acid Battery Guide for Stand-Alone Photovoltaic Systems," *Rep. Int. Energy Agency*, vol. 1, no. December, pp. 1–33, 1999.

[28] "*IEEE Std 1013™-2007: IEEE Recommended Practice for Sizing*

*Lead-Acid Batteries for Photovoltaic (PV) Systems.*" 2007.

[29] D. Zhou, H. Wang, and F. Blaabjerg, "Mission Profile Based System-Level Reliability Analysis of DC/DC Converters for a Backup Power Application," *IEEE Trans. Power Electron.*, vol. 33, no. 9, pp. 8030–8039, 2018.

[30] H. Wang and F. Blaabjerg, "Reliability of Capacitors for DC-Link Applications in Power Electronic Converters—An Overview," *IEEE Trans. Ind. Appl.*, vol. 50, no. 5, pp. 3569–3578, Sep. 2014.

[31] A. Albertsen, "Electrolytic Capacitor Lifetime Estimation," *JIANGHAI Eur. GmbH*, pp. 1–13, 2010.

[32] R. Bayerer, T. Herrmann, T. Licht, J. Lutz, and M. Feller, "Model for Power Cycling Lifetime of IGBT Modules - Various Factors Influencing Lifetime," in *Proc. IEEE CIPS*, 2008, pp. 1–6.

[33] "Technical Information IGBT Modules Use of Power Cycling Curves for IGBT 4," Germany, 2012.

**Saeed Peyghami**, (S'14–M'17) received the B.Sc., M.Sc. and Ph.D. degrees all in electrical engineering, power electronics from the Department of Electrical Engineering, Sharif University of Technology, Tehran, Iran, in 2010, 2012, 2017 respectively. He was a Visiting Ph.D. Scholar with the Department of Energy Technology, Aalborg University, Denmark in 2015 to 2016, where he is currently a Postdoctoral researcher. His research interests include power electronics, microgrids, renewable energies, and reliability.

**Huai Wang**, (M'12, SM'17) received the B.E. degree in electrical engineering, from Huazhong University of Science and Technology, Wuhan, China, in 2007 and the Ph.D. degree in power electronics, from the City University of Hong Kong, Hong Kong, in 2012. He is currently an Associate Professor at the Center of Reliable Power Electronics (CORPE), and Vice Leader of Efficient and Reliable Power Electronics Research Program at Aalborg University, Aalborg, Denmark, and. He was a Visiting Scientist with the ETH Zurich, Switzerland, from Aug. to Sep. 2014, and with the Massachusetts Institute of Technology (MIT), USA, from Sep. to Nov. 2013. He was with the ABB Corporate Research Center, Switzerland, in 2009. His research addresses the fundamental challenges in modelling and validation of power electronic component failure mechanisms, and application issues in system-level predictability, condition monitoring, circuit architecture, and robustness design.

Dr. Wang received the Richard M. Bass Outstanding Young Power Electronics Engineer Award from the IEEE Power Electronics Society in 2016, and the Green Talents Award from the German Federal Ministry of Education and Research in 2014. He is currently the Chair of IEEE PELS/IAS/IE Chapter in Denmark. He serves as an Associate Editor of IET Electronics Letters, IEEE JOURNAL OF EMERGING AND SELECTED TOPICS IN POWER ELECTRONICS, and IEEE TRANSACTIONS ON POWER ELECTRONICS.

**Pooya Davari** (S'11–M'13-SM'19) received the B.Sc. and M.Sc. degrees in electronic engineering from the University of Mazandaran, Babolsar, Iran, in 2004 and 2008, respectively, and the Ph.D. degree in power electronics from Queensland University of Technology (QUT), Brisbane, Australia, in 2013. From 2005 to 2010, he was involved in several electronics and power electronics projects as a Development Engineer. From 2010 to 2014, he investigated and developed high-power high-voltage power electronic systems for multidisciplinary projects, such as ultrasound application, exhaust gas emission reduction, and tissue-materials sterilization. From 2013 to 2014, he was a Lecturer with QUT. He joined as a Postdoctoral Researcher the Department of Energy Technology, Aalborg University, Aalborg, Denmark, in 2014, where he is currently an Associate Professor. His current research interests include EMI/EMC in power electronics, WBG-based power converters, active front-end rectifiers, harmonic mitigation in adjustable-speed drives, and pulsed power applications. Dr. Davari received a research grant from the Danish Council of Independent Research in 2016.

**Frede Blaabjerg** (S'86–M'88–SM'97–F'03) was with ABB-Scandia, Randers, Denmark, from 1987 to 1988. From 1988 to 1992, he got the PhD degree in Electrical Engineering at Aalborg University in 1995. He became an Assistant Professor in 1992, an Associate Professor in 1996, and a Full Professor of power electronics and drives in 1998. From 2017 he became a Villum Investigator. He is honoris causa at University Politehnica Timisoara (UPT), Romania and Tallinn Technical University (TTU) in Estonia.

His current research interests include power electronics and its applications such as in wind turbines, PV systems, reliability, harmonics and adjustable speed drives. He has published more than 600 journal papers in the fields of power electronics and its applications. He is the co-author of four monographs and editor of ten books in power electronics and its applications.

He has received 29 IEEE Prize Paper Awards, the IEEE PELS Distinguished Service Award in 2009, the EPE-PEMC Council Award in 2010, the IEEE William E. Newell Power Electronics Award 2014 and the Villum

Kann Rasmussen Research Award 2014. He was the Editor-in-Chief of the IEEE TRANSACTIONS ON POWER ELECTRONICS from 2006 to 2012. He has been Distinguished Lecturer for the IEEE Power Electronics Society from 2005 to 2007 and for the IEEE Industry Applications Society from 2010 to 2011 as well as 2017 to 2018. In 2018 he is President Elect of IEEE Power Electronics Society. He serves as Vice-President of the Danish Academy of Technical Sciences. He is nominated in 2014, 2015, 2016 and 2017 by Thomson Reuters to be between the most 250 cited researchers in Engineering in the world.